Electronic Supplementary Material (ESI) for Inorganic Chemistry Frontiers.

Supporting Information

NH_2-Modified $\{Eu^{III}_2\}$−Organic Framework for Efficient Chemical Fixation of CO_2 and Highly Selective Sensing of 2,4,6-Trinitrophenol

Hongtai Chen,[a] Zhengguo Zhang,[a] Tuoping Hu,[a] and Xiutang Zhang[a*]

[a]*Department of Chemistry, College of Science, North University of China, Taiyuan 030051, People's Republic of China. E-mail: xiutangzhang@163.com*

Content

Table S1. Crystallographic data and refinement parameters of NUC-41.

Complex	**NUC-41**
Formula	$C_{70}H_{32}Eu_4N_3O_{35}$
Mr	2082.82
Crystal system	orthorhombic
Space group	*P*nma
a (Å)	32.6303(18)
b (Å)	18.587(3)
c (Å)	16.648(5)
α (°)	90
β (°)	90
γ (°)	90
V(Å^3)	10097(3)
Z	4
Dcalcd(g·cm^{-3})	1.370
μ(mm^{-1})	2.520
GOF	0.989
R_1 [I>2σ(I)][a]	0.0584
wR_2 [I>2σ(I)][b]	0.1209
R_1[a] (all data)	0.1094
wR_2[b] (all data)	0.1450
R_{int}	0.1597

[a] $R_1 = \sum| |F_o|-|F_c| | / \sum|F_o|$. [b] $wR_2 = [\sum w(|F_o|^2-|F_c|^2)]/\sum|w(F_o^2)^2|]^{1/2}$

Table S2. Selected bond lengths and angles of NUC-41.

Eu1-O3#1	2.289(7)	Eu1-O5	2.276(7)	Eu1-O8#2	2.491(6)
Eu1-O9#2	2.470(7)	Eu1-O10	2.295(7)	Eu1-O13#3	2.493(6)
Eu1-O14#3	2.384(7)	Eu1-O15	2.313(7)		
Eu2-O2#4	2.382(7)	Eu2-O6#5	2.501(7)	Eu2-O7#5	2.401(6)
Eu2-O11#6	2.312(7)	Eu2-O12	2.243(8)	Eu2-O16	2.279(9)
Eu2-O1W	2.468(9)	Eu2-O14	2.490(6)		
O3#1-Eu1-O8#2	127.5(3)	O3#1-Eu1-O9#2	75.9(2)	O3#1-Eu1-O10	154.1(2)
O3#1-Eu1-O13#3	80.8(2)	O3#1-Eu1-O14#3	87.7(3)	O3#1-Eu1-O15	106.0(3)
O5-Eu1-O3#1	75.8(3)	O5-Eu1-O8#2	151.4(2)	O5-Eu1-O9#2	139.6(3)
O5-Eu1-O10	89.5(3)	O5-Eu1-O13#3	75.4(2)	O5-Eu1-O14#3	128.7(2)
O5-Eu1-O15	80.6(2)	O8#2-Eu1-O13#3	120.4(2)	O9#2-Eu1-O8#2	52.6(2)
O9#2-Eu1-O13#3	127.0(2)	O10-Eu1-O8#2	73.9(2)	O10-Eu1-O9#2	126.4(2)
O10-Eu1-O13#3	74.9(2)	O10-Eu1-O14#3	85.0(3)	O10-Eu1-O15	92.1(2)
O14#3-Eu1-O8#2	74.0(2)	O14#3-Eu1-O9#2	78.1(2)	O14#3-Eu1-O13#3	53.9(2)
O15-Eu1-O8#2	77.0(2)	O15-Eu1-O9#2	80.2(2)	O15-Eu1-O13#3	152.6(2)
O15-Eu1-O14#3	150.5(2)				
O14-Eu2-O6#5	129.8(2)	O2#4-Eu2-O14	54.5(2)	O2#4-Eu2-O65	77.8(3)
O2#4-Eu2-O75	78.5(2)	O2#4-Eu2-O1W	131.9(3)	O75-Eu2-O14	120.6(2)
O7#5-Eu2-O6#5	53.8(2)	O7#5-Eu2-O1W	147.8(3)	O11#6-Eu2-O14	154.9(3)
O11#6-Eu2-O2#4	150.4(3)	O11#6-Eu2-O6#5	73.4(3)	O11#6-Eu2-O7#5	79.3(3)
O11#6-Eu2-O1W	74.8(3)	O12-Eu2-O14	81.5(3)	O12-Eu2-O2#4	82.9(3)
O12-Eu2-O6#5	77.7(3)	O12-Eu2-O7#5	130.6(3)	O12-Eu2-O11#6	97.1(3)
O12-Eu2-O16	148.6(3)	O12-Eu2-O1W	72.2(3)	O16-Eu2-O14	82.3(3)
O16-Eu2-O2#4	108.8(3)	O16-Eu2-O6#5	132.6(3)	O16-Eu2-O7#5	80.8(3)
O16-Eu2-O11#6	86.6(3)	O16-Eu2-O1W	78.8(3)	O1W-Eu2-O14	81.0(3)
O1W-Eu2-O6#5	132.5(3)				
Symmetry transformations used to generate equivalent atoms: #1: 1-X,1/2+Y,1-Z; #2: 3/2-X,1/2+Y,1/2+Z; #3: 3/2-X,1-Y,-1/2+Z; #4: 1/2+X,1/2-Y,3/2-Z; #5: 1/2+X,1/2-Y,1/2-Z; #6: 2-X,1-Y,1-Z.					

Table S3. Comparison of the catalytic performance of NUC-41a catalyst with selected previously reported MOFs.

MOF	Catalyst (mol %)	Temperature	Pressure (MPa)	Time	Yield (%)	Ref.
MOF-205(M)	2.5	RT	0.4	4	80	S1
NH2-MIL-101(Al)	0.17	120	1.8	6	95	S2
MMCF-2	0.13	RT	0.1	48	95	S3
Cr-MIL-101	1.2	RT	0.8	24	82	S4
NUC-41a	0.2	65	0.1	12	98	This work

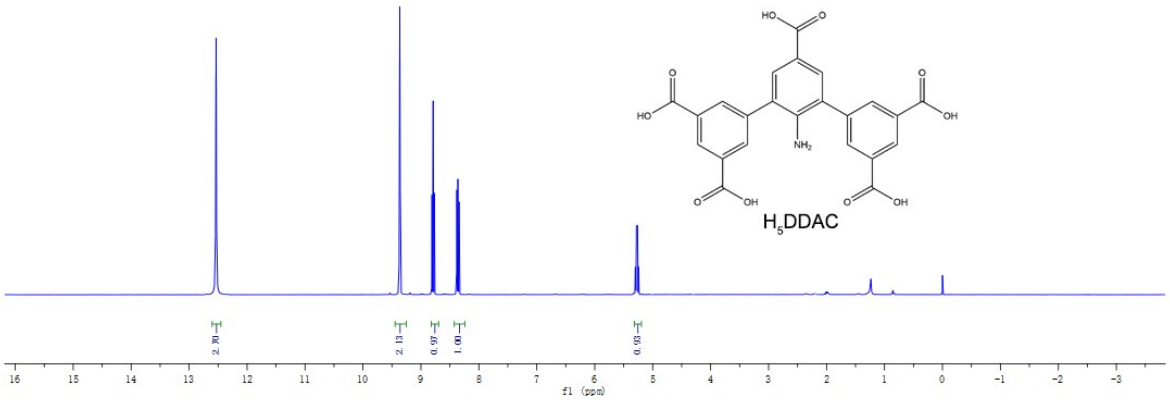

Scheme S1. The ^{1}H NMR of designed H_5DDAC ligand.

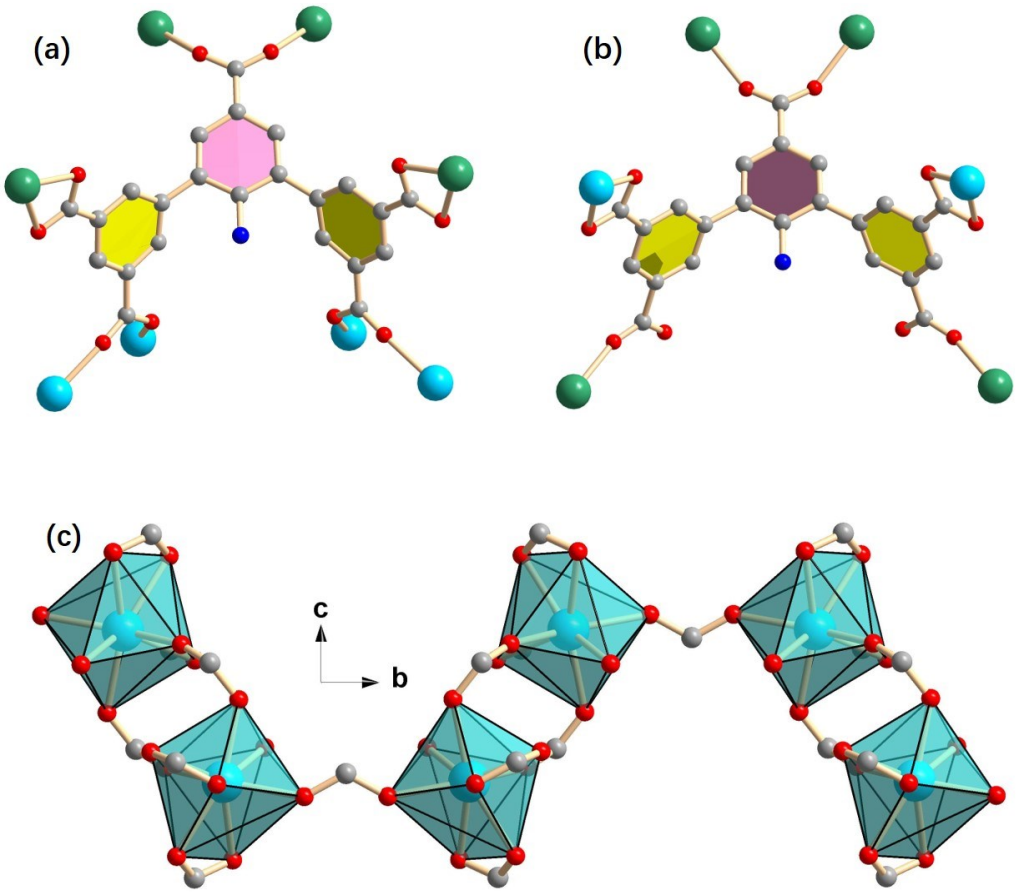

Figure S1. The coordination mode of DDAC ligand with type I (a) and type II (b); the ytterbium-hydroxide structure (b); the one-dimensional $[\{Eu(2)_2\}(HCO_2)]_n$ chain (c).

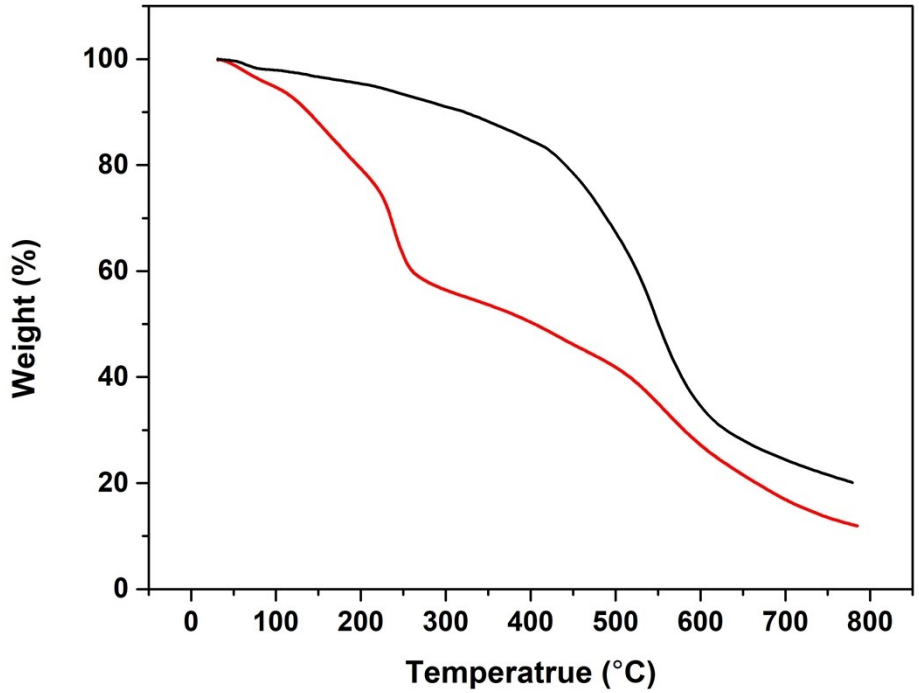

Figure S2. TGA curve of as-synthesized (black) and activated (red) sample of NUC-41.

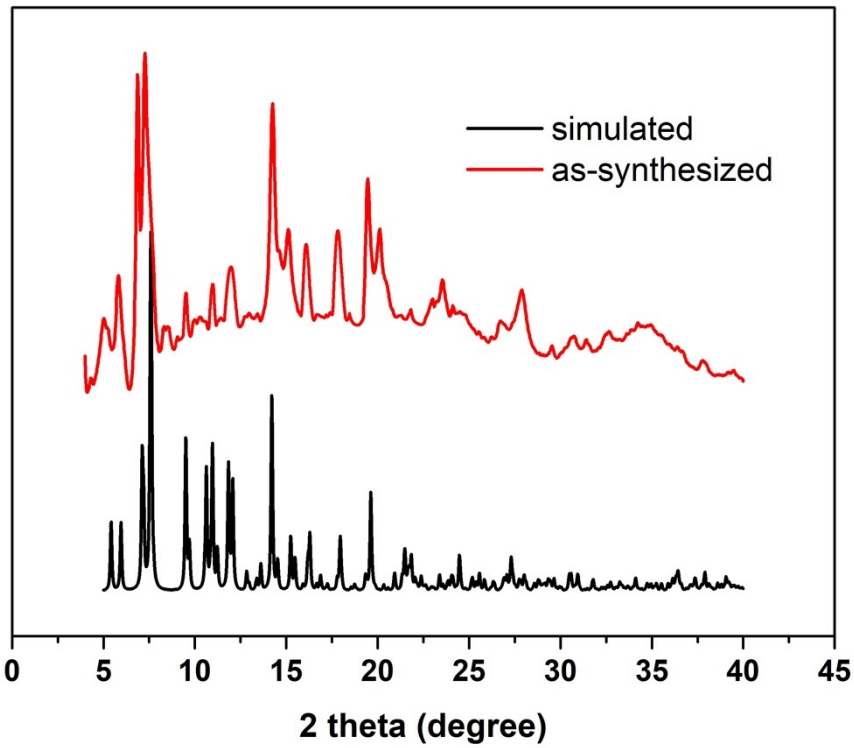

Figure S3. PXRD pattern of as-synthesized NUC-41 sample.

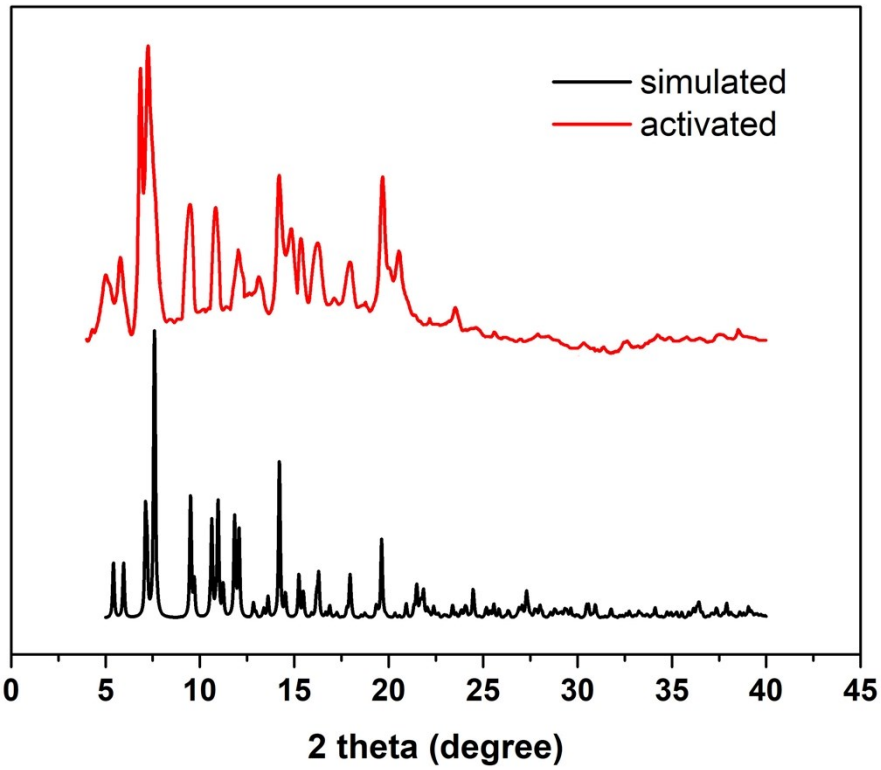

Figure S4. PXRD pattern of NUC-41 after activation.

Isosteric Heat Calculation.

The Q_{st} value is a parameter that describes the average enthalpy of adsorption for an adsorbing gas molecule at a specific surface coverage and is usually evaluated using two or more adsorption isotherms collected at similar temperatures. The zero-coverage isosteric heat of adsorption is evaluated by first fitting the temperature-dependent isotherm data to a virial-type expression, which can be written as:

$$lnP = lnN + \frac{1}{T}\sum_{i=0}^{m} a_i N^i + \sum_{i=0}^{n} b_i N^i \quad (1)$$

$$Q_{st} = -R\sum_{i=0}^{m} a_i N^i \quad (2)$$

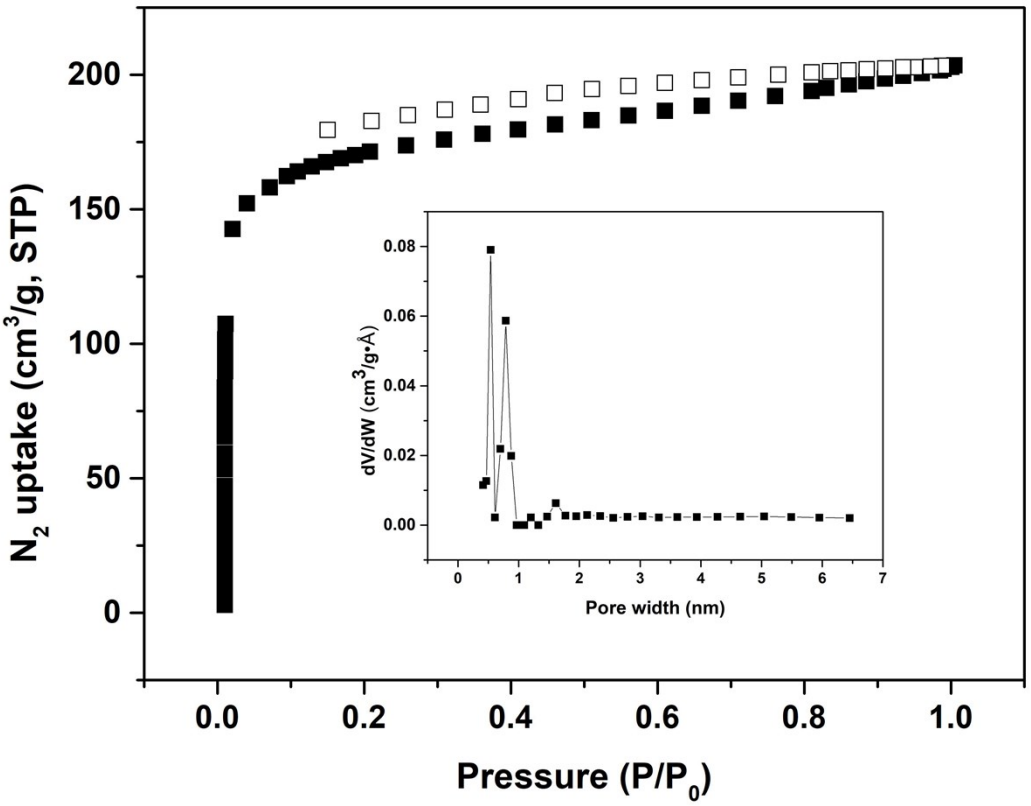

Figure S5. N_2 absorption and desorption isotherms of NUC-41a at 77 K (Insert: the pore size distribution).

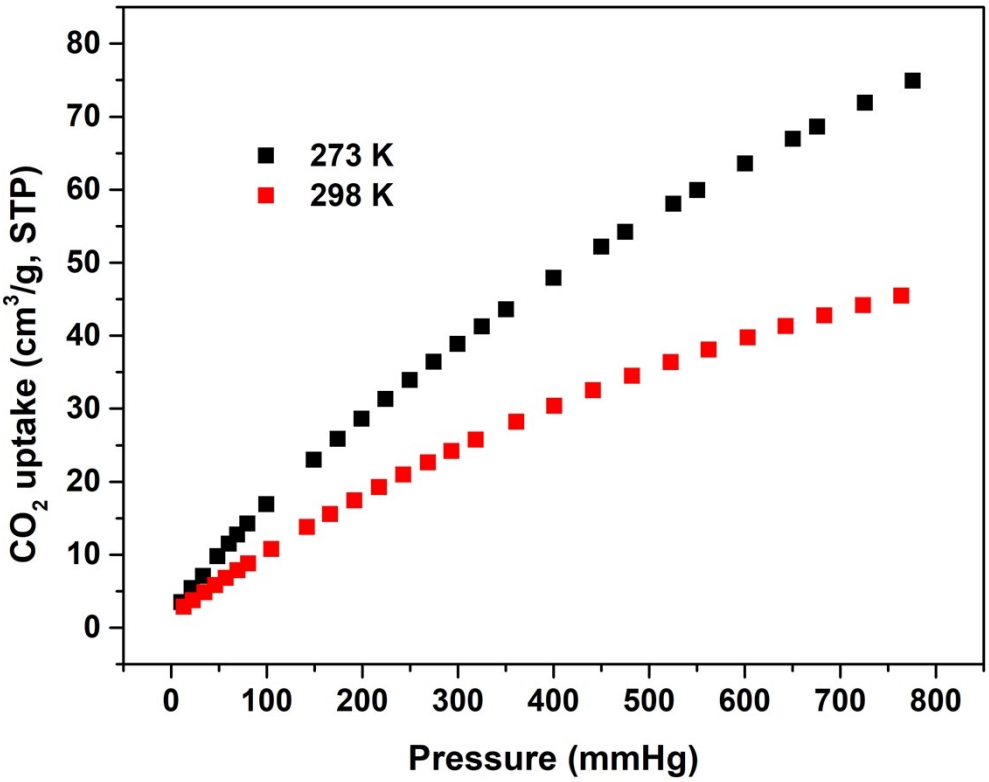

Figure S6. Adsorption isotherm of CO_2 at 273K and 298K.

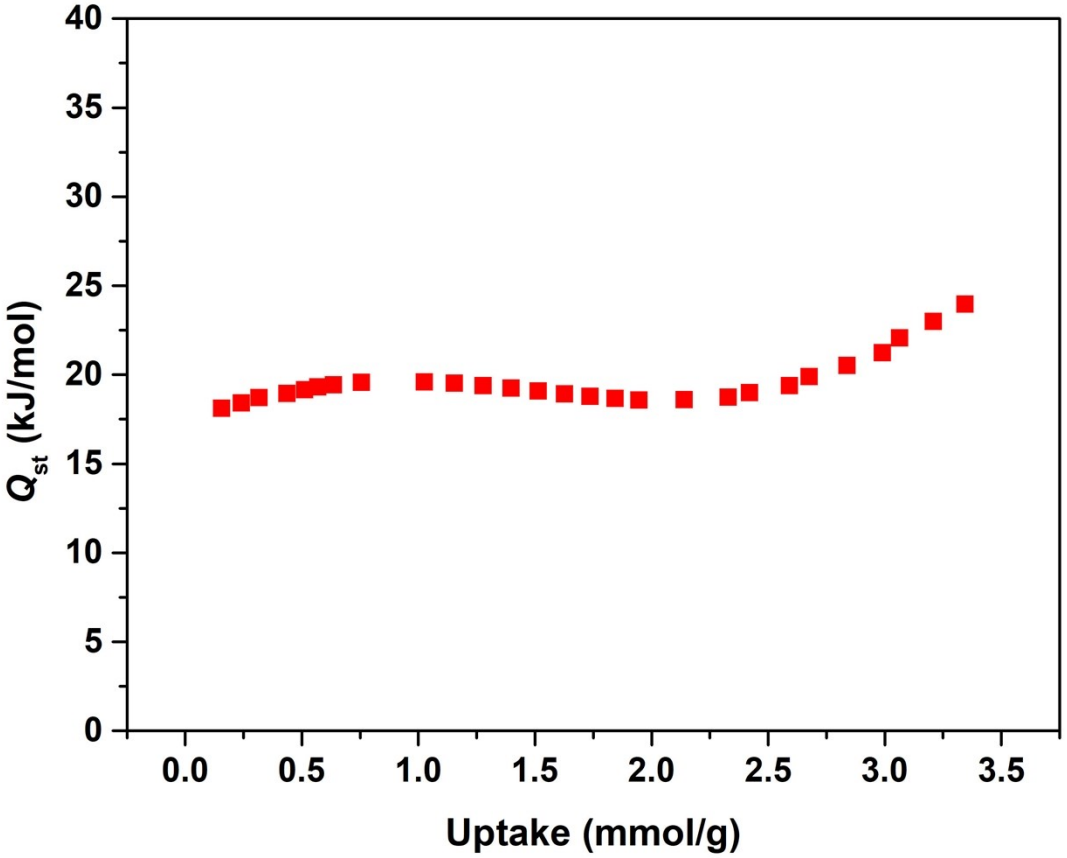

Figure S7. CO_2 adsorption heat calculated by the virial equation of NUC-41a.

Yield Calculation Based on the GC-MS Analysis

Gas chromatography mass spectrometry (GC-MS) analyses were performed on a time-of-flight Thermo Fisher Trace ISQ GC/MS instrument, the yield (%) was calculated based on the consumption of starting material using the equation:

$$Yield\ (\%) = \left(\frac{\frac{area\ of\ reactant\ at\ 0\ hour}{area\ of\ interal\ standard\ at\ 0\ hour} - \frac{area\ of\ reactant\ at\ any\ time}{area\ of\ interal\ standard\ at\ any\ time}}{\frac{area\ of\ reactant\ at\ 0\ hour}{area\ of\ interal\ standard\ at\ 0\ hour}} \right) \times 100\% \quad (3)$$

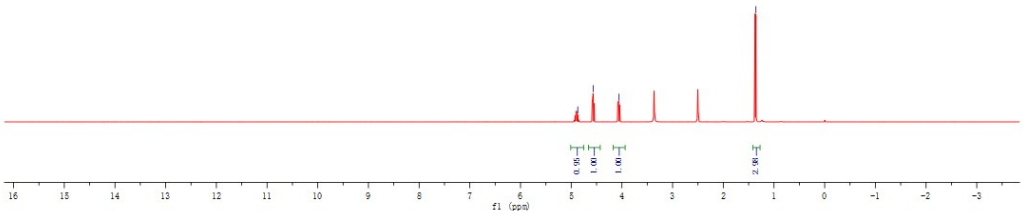

Figure S8. The ^{1}H NMR spectrum of 4-methyl-1,3-dioxolan-2-one (Figure 3, entry 1).

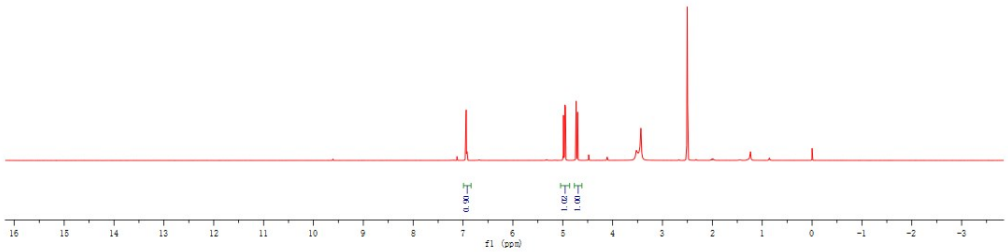

Figure S9. The ^{1}H NMR spectrum of 4-chloro-1,3-dioxolan-2-one (Figure 3, entry 2).

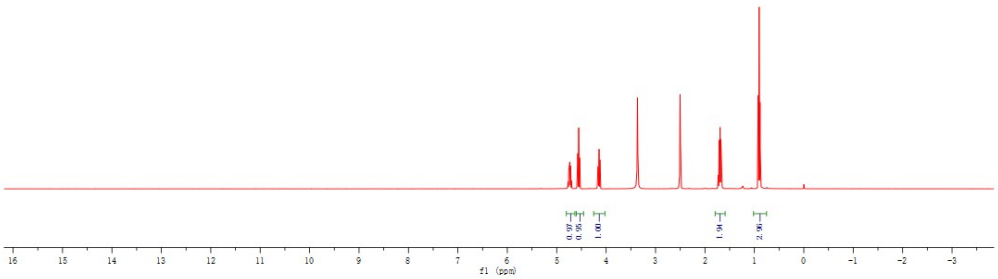

Figure S10. The ^{1}H NMR spectrum of 4-ethyl-1,3-dioxolan-2-one (Figure 3, entry 3).

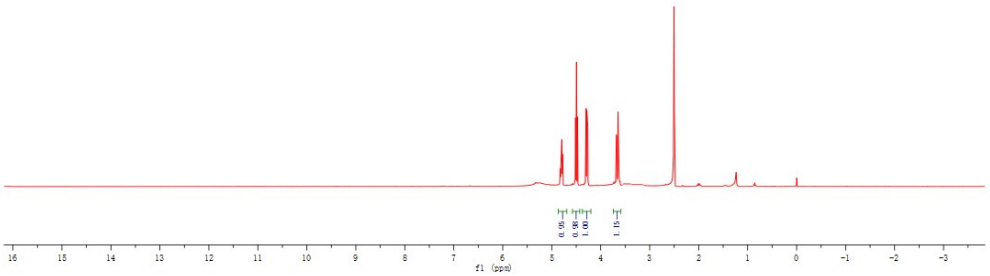

Figure S11. The ^{1}H NMR spectrum of 4-(bromomethyl)-1,3-dioxolan-2-one (Figure 3, entry 4).

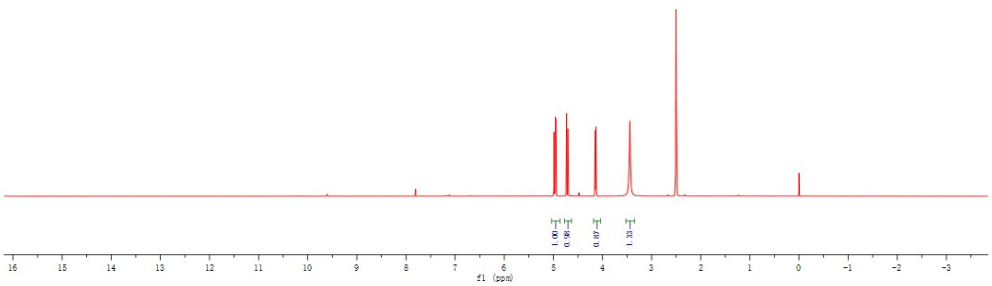

Figure S12. The ^{1}H NMR spectrum of 4-(chloromethyl)-1,3-dioxolan-2-one (Figure 3, entry 5).

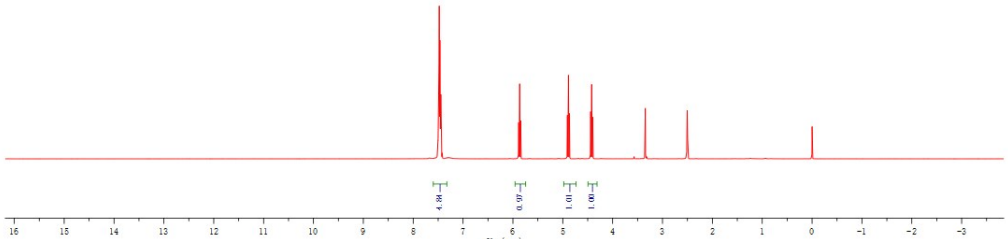

Figure S13. The ^{1}H NMR spectrum of 4-phenyl-1,3-dioxolan-2-one (Figure 3, entry 5).

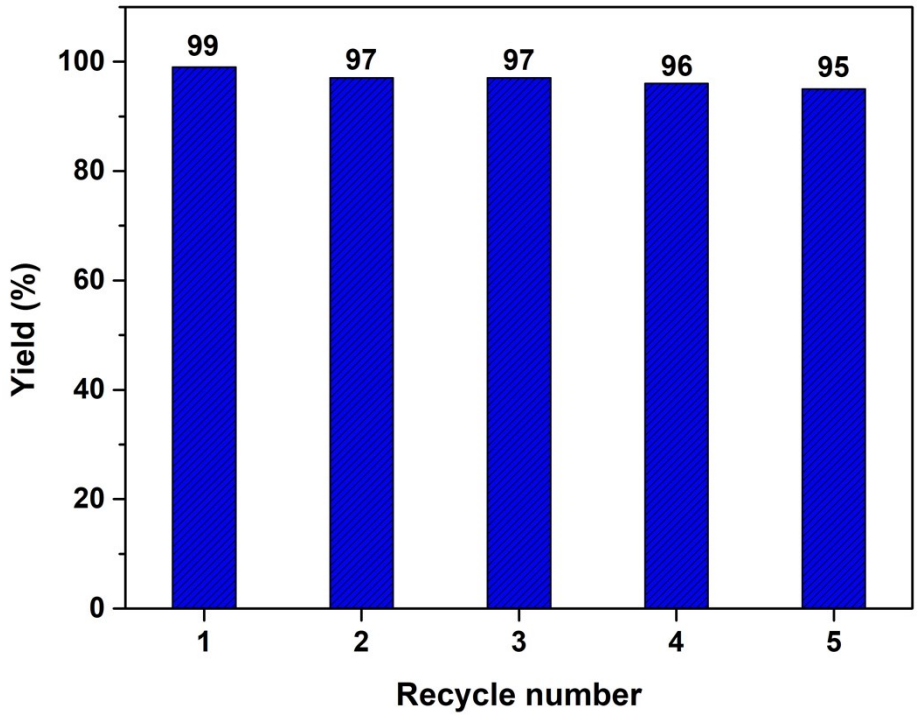

Figure S14. The recycled catalytic cycloaddition reaction.

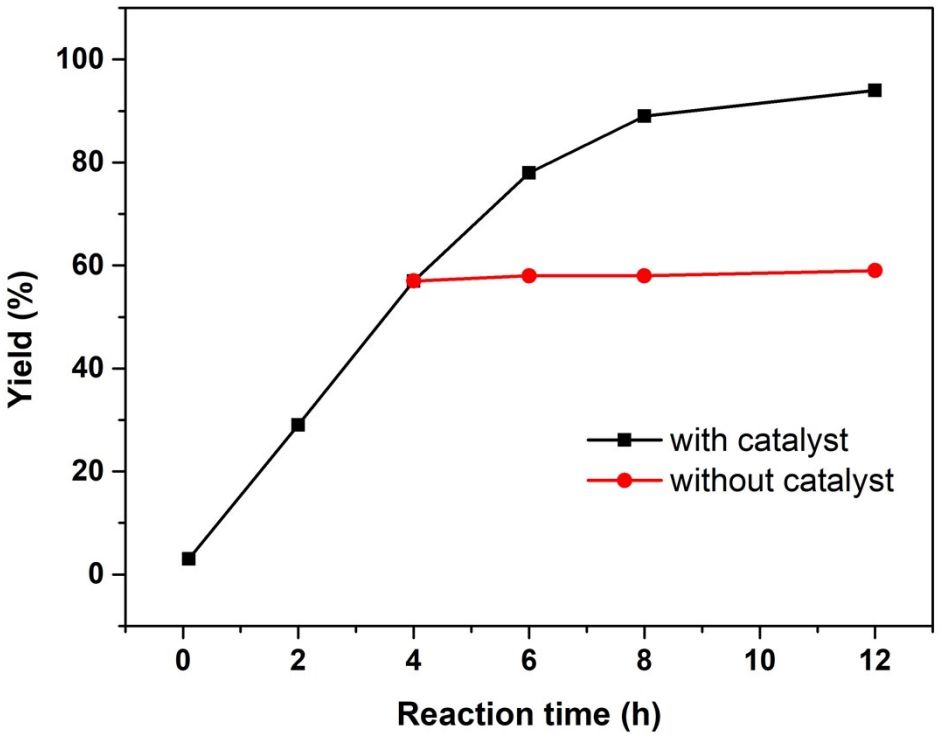

Figure S15. The hot filtration experiment of cycloaddition reaction catalysed by NUC-41a.

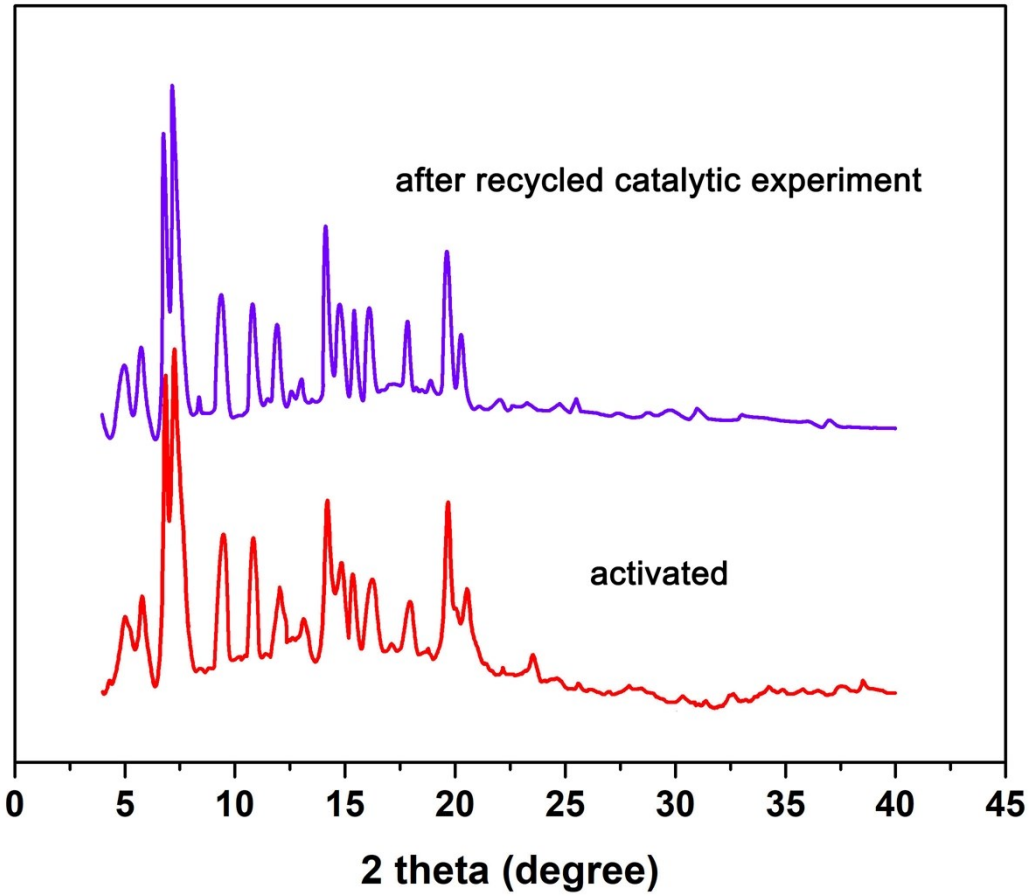

Figure S16. The PXRD pattern of NUC-41a after recycled cycloaddition reaction.

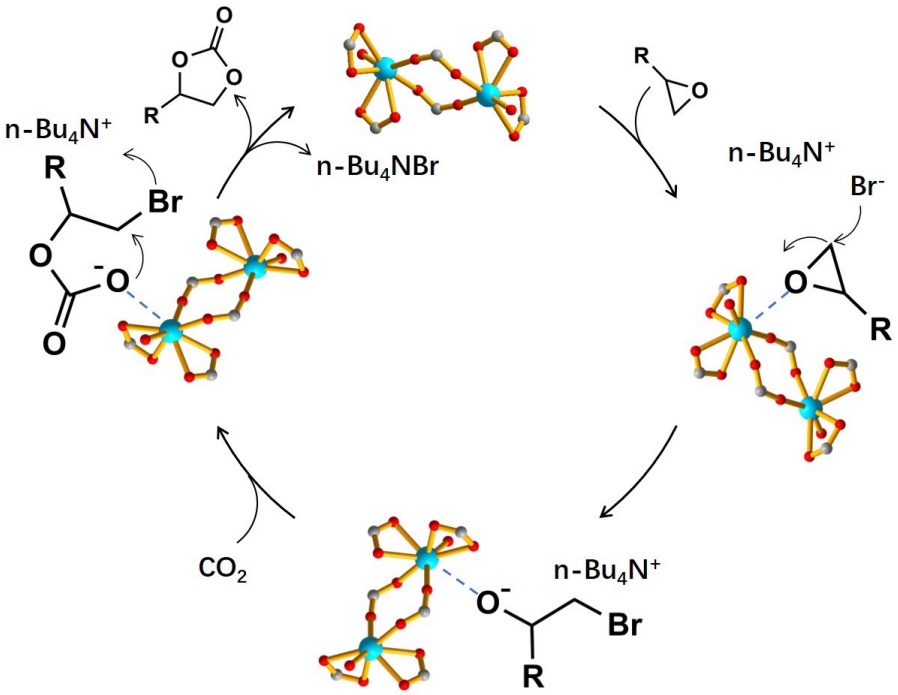

Figure S17. The proposed reaction mechanism for the chemical fixation of CO_2 in presence of synergistic catalysis.

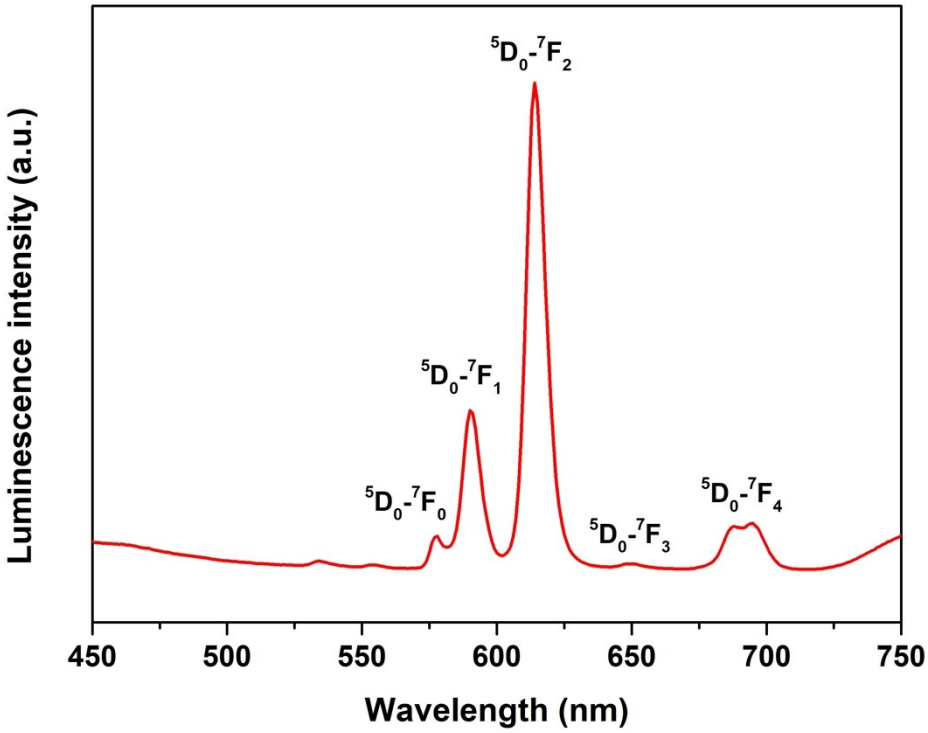

Figure S18. The luminescence spectra of NUC-41.

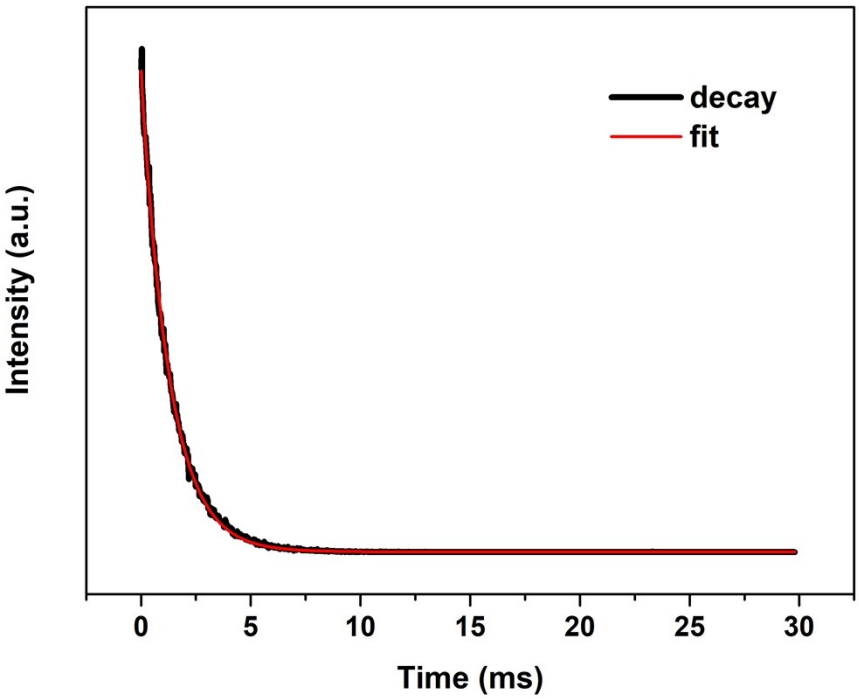

Figure S19. The luminescence lifetime of NUC-41.

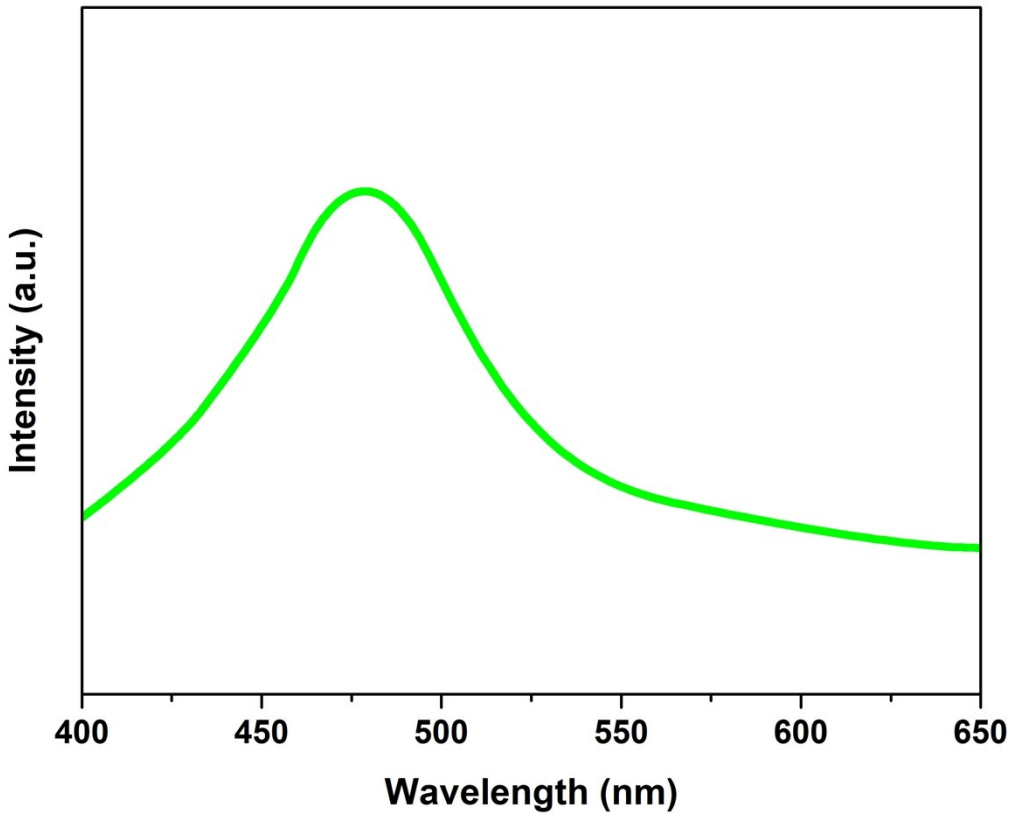

Figure S20. The phosphorescence luminescence of Gd-MOF at 77K.

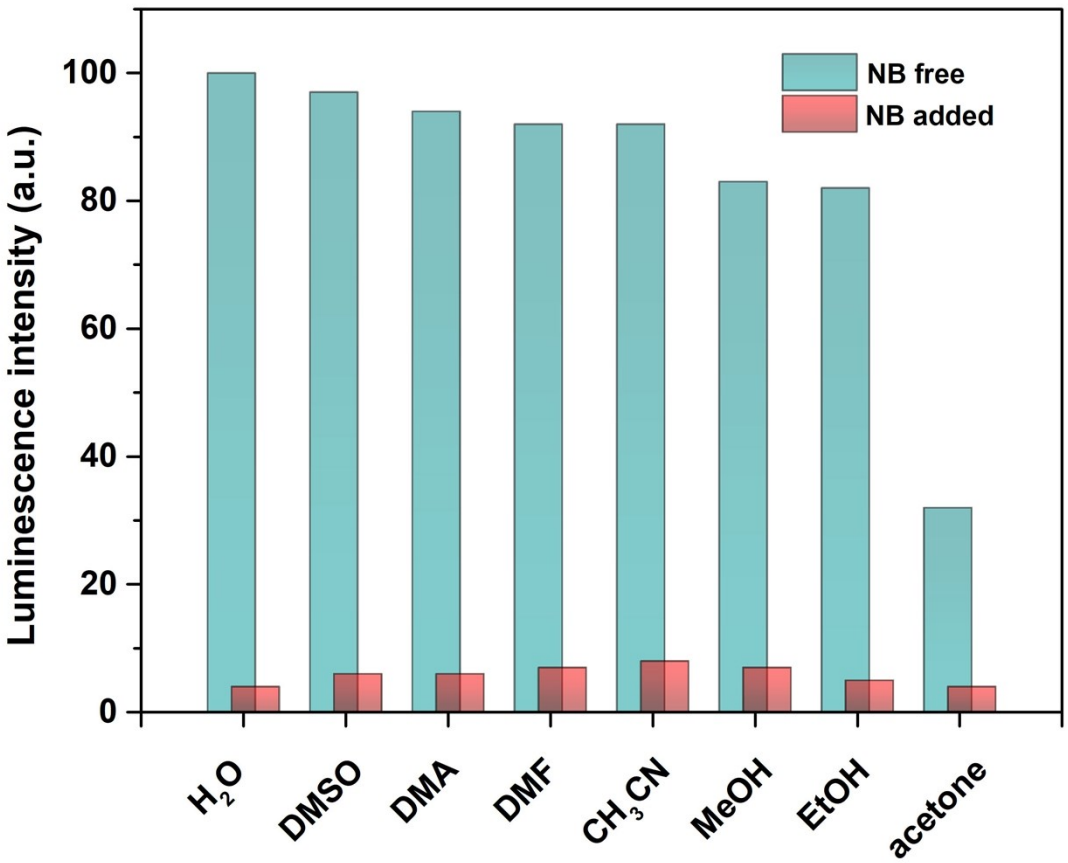

Figure S21. Nitrobenzene-added emission intensity of NUC-41 in the presence of various solvents.

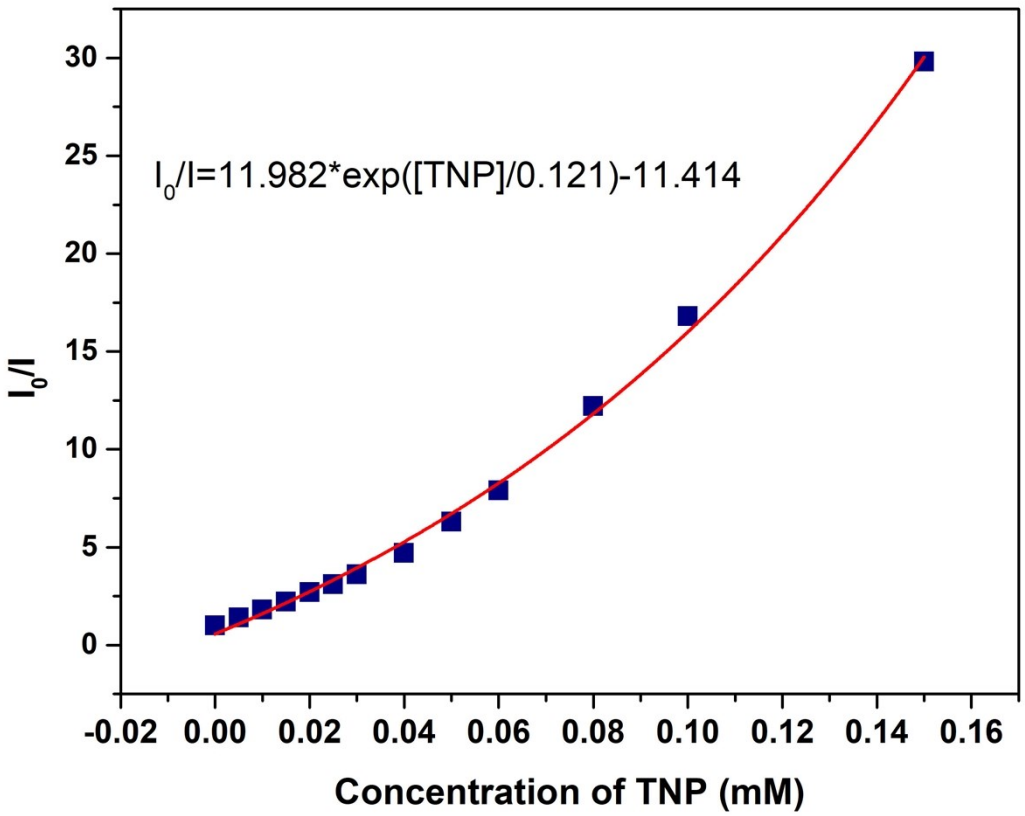

Figure S22. The plot of I_0/I versus the TNP concentration from 0-0.15 mM.

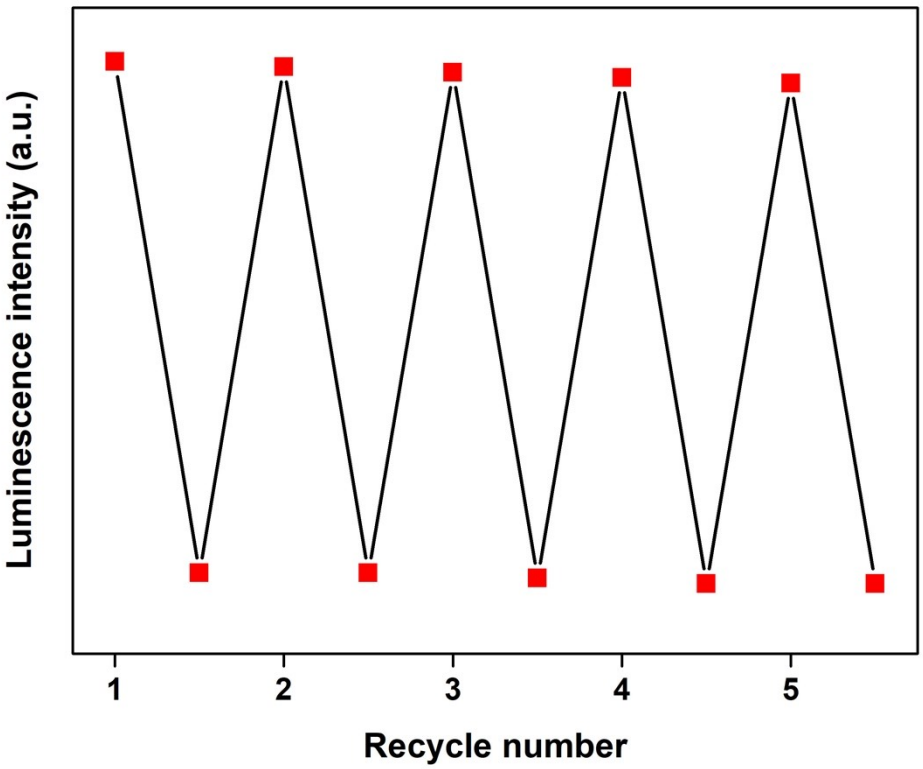

Figure S23. The recycled luminescence sensing experiment of NUC-41 toward TNP.

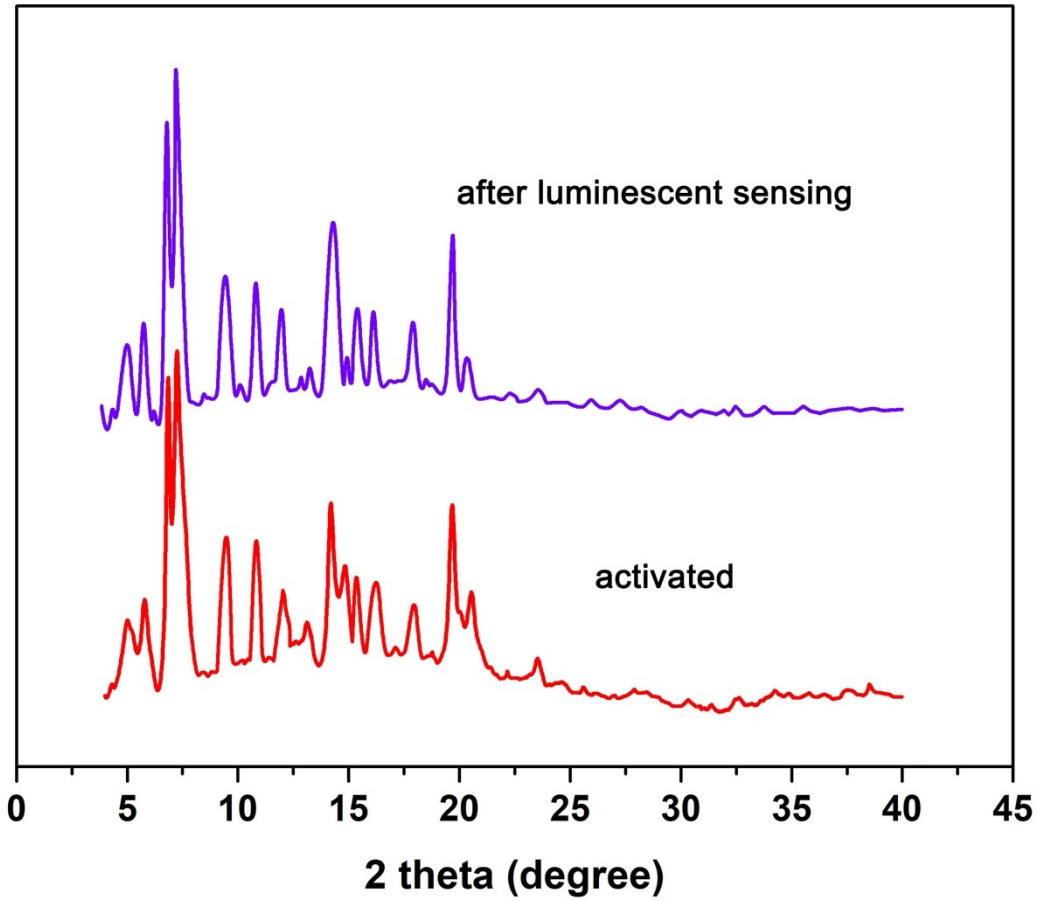

Figure S24. The PXRD pattern of NUC-41 after recycled luminescence sensing of TNP.

Reference

S1. Babu, R. Roshan, R.; Kathalikkattil, A. C.; Kim, D. W.; Park D.-W. Rapid, Microwave-Assisted Synthesis of Cubic, Three-Dimensional, Highly Porous MOF-205 for Room Temperature CO_2 Fixation via Cyclic Carbonate Synthesis. *ACS Appl. Mater. Interfaces* **2016**, *8*, 33723−33731.

S2. Senthilkumar, S.; Maru, M. S.; Somani, R. S.; Bajaj, H. C.; Neogi, S. Unprecedented NH_2-MIL-101(Al)/n-Bu_4NBr System as Solvent-Free Heterogeneous Catalyst for Efficient Synthesis of Cyclic Carbonates via CO_2 Cycloaddition. *Dalton Trans*. **2018**, *47*, 418−428.

S3. Gao, W. Y.; Chen, Y.; Niu, Y. H.; Williams, K.; Cash, L.; Perez, P. J.; Wojtas, L.; Cai, J. F.; Ma, S. Q. Crystal Engineering of an nbo Topology Metal-Organic Framework for Chemical Fixation of CO_2 under Ambient Conditions. *Angew. Chem., Int. Ed*. **2014**, *53*, 2615−2619.

S4. Zalomaeva, O. V.; Chibiryaev, A. M.; Kovalenko, K. A.; Kholdeeva, O. A.; Balzhinimaev, B. S.; Fedin, V. P. Cyclic Carbonates Synthesis from Epoxides and CO_2 Over Metal−organic Framework Cr-MIL-101. *J. Catal*. **2013**, *298*, 179−185.